

MambaCapsule: Towards Transparent Cardiac Disease Diagnosis with Electrocardiography Using Mamba Capsule Network

Yinlong Xu^a, Xiaoqiang Liu^b, Zitai Kong^a, Yixuan Wu^c, Yue Wang^d, Yingzhou Lu^f, Honghao Gao^{g,h}, Jian Wu^c and Hongxia Xu^{e,*}

^aCollege of Computer Science & Technology, Zhejiang University, Hangzhou, China

^bDepartment of Gastroenterology, First Hospital of Quanzhou Affiliated to Fujian Medical University, Quanzhou, China

^cSchool of Public Health, Zhejiang University, Hangzhou, China

^dState Key Laboratory of Transvascular Implantation Devices of The Second Affiliated Hospital and Liangzhu Laboratory, Zhejiang University School of Medicine, Hangzhou, China

^eInnovation Institute for Artificial Intelligence in Medicine, Zhejiang University, Hangzhou, China

^fSchool of Medicine, Stanford University, USA

^gSchool of Computer Engineering and Science, Shanghai University, Shanghai, China

^hCollege of Future Industry, Gachon University, Korea

ARTICLE INFO

Keywords:

Mamba

Capsule

ECG Classification

Explainable AI

ABSTRACT

Cardiac arrhythmia, a condition characterized by irregular heartbeats, often serves as an early indication of various heart ailments. With the advent of deep learning, numerous innovative models have been introduced for diagnosing arrhythmias using Electrocardiogram (ECG) signals. However, recent studies solely focus on the performance of models, neglecting the interpretation of their results. This leads to a considerable lack of transparency, posing a significant risk in the actual diagnostic process. To solve this problem, this paper introduces MambaCapsule, a deep neural networks for ECG arrhythmias classification, which increases the explainability of the model while enhancing the accuracy. Our model utilizes Mamba for feature extraction and Capsule networks for prediction, providing not only a confidence score but also signal features. Akin to the processing mechanism of human brain, the model learns signal features and their relationship between them by reconstructing ECG signals in the predicted selection. The model evaluation was conducted on MIT-BIH and PTB dataset, following the AAMI standard. MambaCapsule has achieved a total accuracy of 99.54% and 99.59% on the test sets respectively. These results demonstrate the promising performance under the standard test protocol.

1. Introduction

Cardiac arrhythmia refers to the disruption of the cardiac rhythm caused by abnormal cardiac electrical activity (Khraishah et al., 2022). For the reason that arrhythmia serves as an indicator to advent heart consequence, its accurate detection and classification are imperative for mitigating potential risks and complications. Electrocardiogram (ECG) is widely used for recording the electrical cardiac activity (Faust et al., 2013). It provides critical information about the cardiac function and health by measuring the cardiac electrical signals during each heartbeat cycle, which makes it a reliable tool for diagnosing heart health.

Recent researches have shown great advantages of deep learning in arrhythmia classification (Krittanawong et al., 2017; Luz et al., 2016), leveraging the information contained in ECG signals. The development of powerful and effective deep learning methods has the potential to significantly improve the accuracy and efficiency of arrhythmia diagnosis, and ultimately leads to better patient outcomes.

Although the numerous previous models have made substantial progress in arrhythmia classification, most of them solely focus on the performance neglecting the interpretation of their results, which leads to a considerable lack of transparency and poses a low reliability in the actual diagnostic process (Yildirim et al., 2018).

To alleviate this limitation, we proposed a encoder-decoder based neural network called **MambaCapsule** in this paper. Inspired by the mechanism of brain processing (Luppi et al., 2024; Bao et al., 2017; Wang et al., 2021), which tells what features exactly the eyes see and tells the reason why the brain chooses to classify one item to this label not the other one, we novelly designed our model to implement both processes by using the main architecture for prediction and a reconstruct part for explanation. Our evaluation was carried on MIT-BIH dataset (Moody and Mark, 2001) and PTB (Bousseljot et al., 1995) dataset, reached 99.54% and 99.59% accuracy. By applying a reconstruct network, we could intuitively know what the model sees and why it makes that decision.

The main contributions of this paper are as follows:

- We introduced a novel encoder-decoder based network architecture based on **Mamba** (Gu and Dao, 2023) and **Capsule networks** (Sabour et al., 2017), changing the form of the output from the probability

*Corresponding author

✉ 22321336@zju.edu.cn (Y. Xu); liuxiaoqianghusina@163.com (X.

Liu); kongzitai@zju.edu.cn (Z. Kong); wyx_chloe@zju.edu.cn (Y. Wu);

ywang2022@zju.edu.cn (Y. Wang); lyz66@stanford.edu (Y. Lu);

gaohonghao@shu.edu.cn (H. Gao); honghaogao@gachon.ac.kr (H. Gao);

wujian2000@zju.edu.cn (J. Wu); Einstein@zju.edu.cn (H. Xu)

ORCID(s): 0009-0008-1987-7562 (Y. Xu)

sequence to capsule vector sequence, which contains both the classification and feature attribute.

- We applied a downstream network to reconstruct the ECG signal. The reconstructed signal can be used to explain what our model learns and the reason why our model makes its prediction.
- We applied a fusion states SSM architecture in process of feature extraction. The evaluation indicators show the feature extracted has considerable advantages on the MIT-BIH and PTB datasets.

2. Related work

2.1. Mamba Nerual Network

Mamba has made excellent performance in numerous traditional fields since it was proposed by Gu and Dao (2023). Different from traditional and the most popular structure Transformer, the advantages of Mamba are mainly reflected in the computational efficiency and the ability to deal with long sequences. For the reason above, many researches have been carried to replace traditional components with Mamba. Wang et al. (2024a) proposed Graph-Mamba, which improved the remote context modeling ability of attention mechanism by integrating Mamba block and node selection mechanism, and solved the problems of high computing cost and limited scalability of attention mechanism. Rimon et al. (2024) proposes a new model-based meta-reinforcement learning method, achieving higher returns and better sample efficiency (up to 15x) with little need for hyper-parameter tuning. Qiao et al. (2024) proposes a multi-modal large language model VL-Mamba based on state space model, demonstrating competitive performance on a variety of multi-modal benchmark tasks and the great potential of state-space models in multi-modal learning.

Mamba also show its advantages in vision tasks (Wang et al., 2024b; Ma et al., 2024; Liu et al., 2024). Zhu et al. (2024) proposed a generic vision backbone with bidirectional Mamba blocks (Vim) to solve the location sensitivity and global context requirements of visual data. Vim performs well in various tasks, with significant improvements in compute and memory efficiency. Li et al. (2024) introduced VideoMamba into video understanding task. Its linear-complexity operator enables efficient long-term modeling, which is crucial for high-resolution long video understanding.

2.2. Capsule Neural Network

Capsule network was first proposed in a 2D handwritten digital image classification task and has excellent performance in the view-invariance (Sabour et al., 2017). Later on, it was widely applied to point cloud (Zhao et al., 2019), image processing (Chen et al., 2021a; Vijayakumar, 2019), and tabular learning (Chen et al., 2023), graph learning (Xinyi and Chen, 2018). Specifically, (Xiang et al., 2018) proposed a multi-scale capsule network that is more robust and efficient for feature representation in image classification,

demonstrating a competitive performance on FashionM-NIST and CIFAR10 datasets. Nguyen et al. (2019) introduce a capsule network that can detect various kinds of attacks. The model uses many fewer parameters than traditional convolutional neural networks with similar performance.

Capsule neural network also has a intrinsic advantage for explaining its results. For instance, Li et al. (2019a) produced a sentiment capsule to identify the informative logic unit and the sentiment based representations in user-item level for rating prediction. By introducing capsules in different layers, Shahroudnejad et al. (2018) demonstrated the possibility of transforming deep networks into transparent networks. This work helps make DNNs' internal processes more understandable and provides the ability to explain their decisions.

2.3. ECG based Cardiac Disease Diagnosis

Numerous researches have been carried in the field of ECG signal classification and the most challenging part of it is to extract the features from the signal. The feature extraction methods have experienced from the manual features and automatic features. Manually designed features extracting usually applied by traditional ML methods like Support Vector Machine (Qin et al., 2017b) and Random Forest (Rouhi et al., 2021). Qin et al. (2017a) proposed an effective methods to extract the abnormal beat eigenvectors of low-dimensional ECG and classify them using support vector machine. Majeed and Alkhafaji (2023) proposed a ML model using multi-domain features combined with least-square support vector machine (LS-SVM), which extracts the time and frequency domain features and selects the most relevant ones.

With the success of deep learning in vision and NLP fields, its ability has been admitted and has been applied to many other fields, including the ECG signal classification (Chen et al., 2022, 2024; Hu et al., 2024; Hong et al., 2019; Ribeiro et al., 2020; Pyakillya et al., 2017; Bian et al., 2022; Chen et al., 2021b; Yan et al., 2019). Li et al. (2020) proposed a 1D residual CNN based on deep residual networks with a 31-layer one-dimensional residual convolutional neural network combined with 2-lead ECG signals for the classification. Kim et al. (2022) proposed a novel model combining residual networks, compressed activation blocks and bidirectional short-duration memory networks. It was evaluated on multiple databases and the results showed that the framework performed well especially for a small number of categories.

Although these methods have their own way to explain the process of the prediction, their lack of accuracy and inadequacy of features extracting hinder their practical applications. Some efforts also focused on the class imbalance problem on ECG datasets. For instance, El-Ghaish and Eldele (2024) introduced a deep learning model called ECGTransForm, which combines multi-scale convolution, channel calibration module and two-way Transformer mechanism to improve the ability to capture spatio-temporal features in ECG data and solves class imbalance problem by introducing context-aware loss function. However, these

methods were employed through simple data reinforcement using statistical methods, the reinforced data benefits to model performance but has no specific physiological information through the process of the reinforcement.

3. Methods

3.1. Mamba

State space models (SSMs) Gu et al. (2021); Gu (2023) are defined as 1D-time-invariant systems, which serve as the predecessor of Mamba. These systems aim to map a 1D input sequence $x(t) \in \mathbb{R}^L$ to a 1D output sequence $y(t) \in \mathbb{R}^L$ through a hidden state $h(t) \in \mathbb{R}^N$, which can be represented as the following equations:

$$\begin{aligned} h(t) &= Ah(t) + Bx(t) \\ y(t) &= Ch(t) \end{aligned} \quad (1)$$

where $A \in \mathbb{R}^{N \times N}$, $B \in \mathbb{R}^{N \times L}$, $C \in \mathbb{R}^{L \times N}$. Considering that deep neural networks operate in discrete space, researchers applied a zero-order preservation on the matrix A and B , turning the equations to the form as:

$$\begin{aligned} h_t &= \bar{A}h_{t-1} + \bar{B}x_t \\ y_t &= Ch_t \end{aligned} \quad (2)$$

Where $\bar{A} = \exp(\Delta A)$ and $\bar{B} = (\Delta A)^{-1}(\exp(\Delta A) - I) \cdot (\Delta B)$ for Δ represents the time step in the continuous space. SSMs also code the remote dependency by initializing matrix A as HiPPO(Gu et al., 2020) and allow training in the form of a convolution kernel to accelerate the training process. However, the matrix A , B and C do not change whatever the input data are, leading to problem of low sensitivity. To solve the problem, Mamba applies a selective method to SSMs, which makes the matrix B and C and Δ adapt themselves based on the input as follows:

$$\begin{aligned} \bar{B} &= s_B(x) \\ \bar{C} &= s_C(x) \\ \bar{\Delta} &= \tau_{\Delta}(\text{Parameter} + s_A(x)) \end{aligned} \quad (3)$$

Where s_B , s_C and s_A are linear projections, and τ_{Δ} is a SoftPlus function. The matrix A does not depend on the input directly, it is influenced by the $\bar{\Delta}$ in the process of the zero-order preservation, making all main parameter inputs adaptable(Gu and Dao, 2023).

3.2. Capsule Networks

The whole network contains three parts: the convolution network, the capsule network and the dynamic routing. The difference between the capsule network and the traditional neural network is that the unit of the neural network is a scalar neuron $x \in \mathbb{R}$, while the unit of the capsule network is a capsule, which is a vector $x \in \mathbb{R}^N$.

In a capsule network, there are many capsules in one layer, and each capsule contains two types of information: the given vector's orientation and the vector's length as the

probability of the capsule, the next capsule first applies a linear transformation of the previous capsule output as:

$$\hat{u}_{j|i,L+1} = W_{ij,L}u_{i,L} \quad (4)$$

where $u_{i,L} \in \mathbb{R}^D$ is the i -th output capsule at layer L , $W_{ij,L} \in \mathbb{R}^{\hat{D} \times D}$ serves as the transformation matrix and the $\hat{u}_{j|i,L+1} \in \mathbb{R}^{\hat{D}}$ represents the contributes from the parent i -th capsule to the j -th one at layer $L + 1$. The model then gets the weight of each contributes through a clustering like routing algorithm. At present, the popular routing algorithms include dynamic routing algorithm and self-routing algorithm. This paper adopts dynamic routing algorithm, which obtains the final weight coefficient through several rounds of iteration. In each iterations, the weight coefficient c is:

$$c_{ij} = \frac{\exp(b_{ij})}{\sum_k \exp(b_{ik})} \quad (5)$$

In the first iteration the b_{ij} is initialized to 0 and will be updated at the end of each iteration. Then the coefficient is used to calculate the temp capsule:

$$s_j = \sum_i c_{ij}\hat{u}_{j|i} \quad (6)$$

Where $s_j \in \mathbb{R}^{\hat{D}}$ serves as a temp result for an iteration, the capsule network designs a special activation function to transform the length of the capsule into [0-1] as:

$$v_j = \frac{\|s_j\|^2}{1 + \|s_j\|^2} \frac{s_j}{\|s_j\|} \quad (7)$$

Where $v_j \in \mathbb{R}^{\hat{D}}$ serves as the real output capsule in each iteration. The equation 7 separates the long and short length of the capsules in the dim of 0 to 1, making the long capsule close to 1 and short capsule close to 0. Then the b_{ij} is updated as:

$$b_{ij} = b_{ij} + v_j\hat{u}_{j|i} \quad (8)$$

The equation 8 serves as an clustering-like algorithm for after each iteration the b_{ij} grows bigger in capsule whose position is closest to the others. And after the setting iterations have done, the v_j will serve as the output of the capsule networks.

3.3. Model Architecture

In this section, we present a classification model based on Mamba and Capsule networks. The overall framework, as shown in Figure 1, consists of three main parts: the feature network, the capsule network and the reconstruction network. Before be fed into the feature network, the input ECG signal is firstly up-projected to contain scope knowledge not a signal sequence, the input shape changes from $x \in \mathbb{R}^{\text{batch,length}}$ to $\hat{x} \in \mathbb{R}^{\text{batch,length,dim}}$.

Then N Mamba Layers constitute a pipeline to extract features from the \hat{x} and each Layer contains a Mamba Block

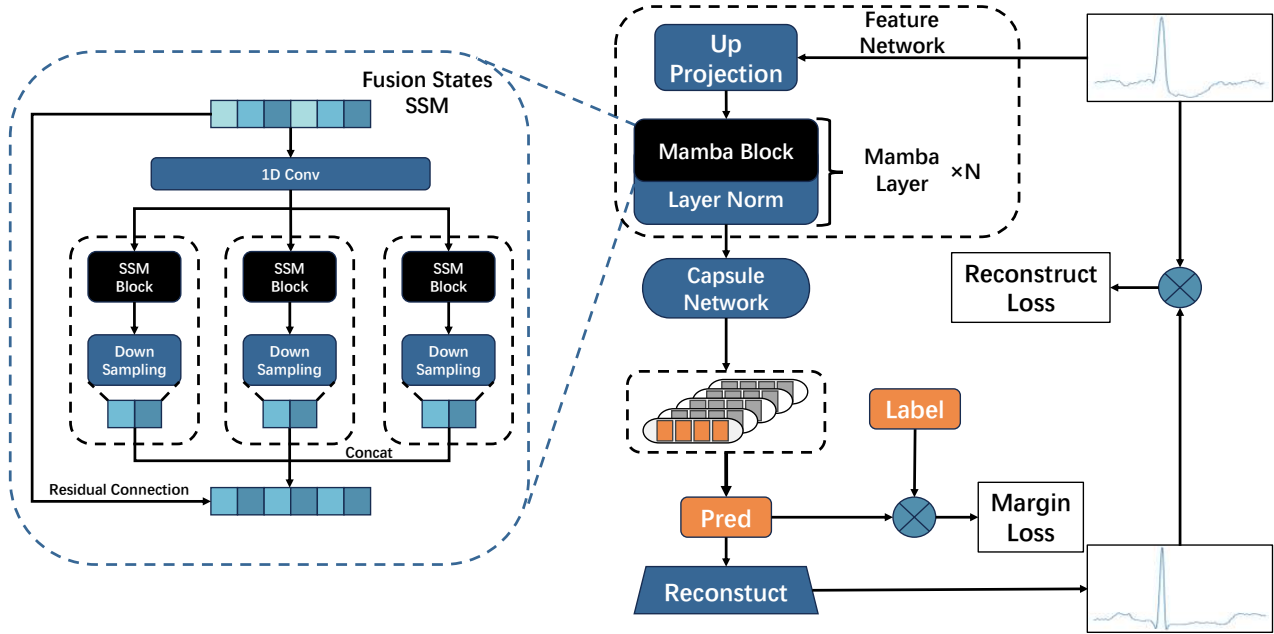


Figure 1: The architecture of MambaCapsule. The model consists of three main parts: the feature network, the capsule network and the reconstruction network. We propose a fusion states SSM to construct backbone of the feature network.

and a Layer Norm. Previous work typically apply a single state Mamba as the encoder backbone, however, these fails to extract wider and narrower features. To solve this problem, we propose a fusion states SSM to construct the Mamba Block. For the i -th Block, it first applies a 1D-convolution on the upstream $i-1$ -th feature sequence x_i , which does not change the dimension of the sequence. Then the sequence will be handled by m different SSM Blocks. The different SSM Blocks focus on different scales of time step and have different convolution shape to obtain more abundant and wider features. Then the features will be down sampled and then linked together to add the x_i in the same shape. The whole process can be formulated as:

$$\begin{aligned}
 \hat{x}_i &= Conv_{1D}(x_i) \\
 u_j &= DownSample_j(SSM_j(\hat{x}_i)) \\
 x_{i+1} &= Concat\left(\sum_j^m u_j\right) + x_i
 \end{aligned} \tag{9}$$

Where $u_j \in \mathbb{R}^{batch, length, dim/m}$ and the m is the factor of the dim to assure $x_{i+1} \in \mathbb{R}^{batch, length, dim}$.

The feature network extracts the signal features and sends the features to the capsule network. The capsule network outputs it in the form of capsules in the end.

The loss of our model consists of two parts, the marginal loss of focusing on model output and the label, and the reconstruct loss focusing on the reconstructed signal and the original signal.

Since our output is in the form of a capsule network, we must first take the geometric length of the output as the probability of the classification label, and then the difference between the set positive label threshold and negative label threshold is made. The final form of margin loss function is as follows:

$$\begin{aligned}
 Loss_{margin} &= \sum_k T_k \max(0, m^+ - ||v_k||)^2 + \\
 &\quad \lambda(1 - T_k) \max(0, ||v_k|| - m^-)^2
 \end{aligned} \tag{10}$$

Where $v_k \in \mathbb{R}^D$ is the k -th output capsule represents one class of the classification, $T_k = 1$ if the label of the input is k , and $m^+ = 0.9$, $m^- = 0.1$ at the beginning. λ is used to prevent the lengths of vectors from shrinking too much, which is set to 0.5 in the beginning.

Reconstruct loss needs to choose the label with the highest probability or we choose it for other reasons. Then we put the output into the reconstruct model, which is a 3 fully connection layers model with Relu activation. After that, calculate the MSE loss of the reconstructed signal output of the reconstruct model and the original input signal, the reconstruct loss is formulated as follows:

$$\begin{aligned}
 \hat{x}_{reconstruct} &= Model(v_{choose}) \\
 Loss_{reconstruct} &= MSELoss(\hat{x}_{reconstruct}, x_{origin})
 \end{aligned} \tag{11}$$

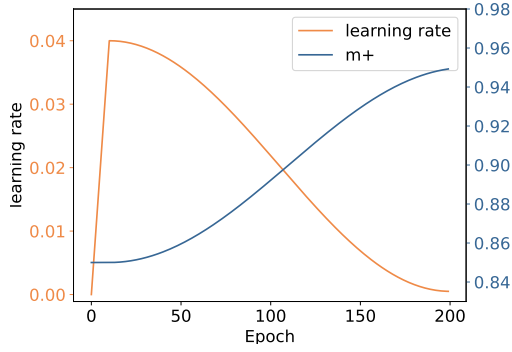


Figure 2: Training set about learning rate and m^+

4. Model setup and Evaluation

4.1. Training Strategy

Since the output probability density of the capsule network is not the same as that of the traditional neural classification network, and the bias can directly affect the output, we adjusted bias by cosine schedule during the training process, so that the threshold of bias kept increasing. At the same time, due to the slow training speed of capsule network in the initial stage of training, the cosine annealing algorithm after linear increase is adopted to change the learning rate. The changes of bias and learning rate are shown in the figure.2

4.2. Performance Metrics

To evaluate the model, we applied five performance indexes: accuracy(ACC), sensitivity (SEN), F1-score(F1), precision (PPV) and specificity (SPEC). These indexes are defined as follows:

$$\begin{aligned}
 ACC &= \frac{TP + TN}{TP + TN + FP + FN} \\
 SEN &= \frac{TP}{TP + FN} \\
 F1 &= 2 \times \frac{ACC \times SEN}{ACC + SEN} \\
 PPV &= \frac{TP}{TP + FP} \\
 SPEC &= \frac{TN}{TN + FP}
 \end{aligned} \tag{12}$$

In these formulas, TP represents the number of true positives (correctly labeled positive); TN represents the number of true negatives (correctly labeled negative); FP represents the number of false positives (incorrectly labeled positive); and FN represents the number of false negatives (incorrectly labeled negative).

4.3. Dataset

Our training and testing datasets are preprocessed in the same routine and are randomly splited in a ratio of 0.8. The detailed description of the dataset is in Table 1:

4.3.1. MIT-BIH Arrhythmia Dataset

The MIT-BIH arrhythmia dataset (Moody and Mark, 2001) is widely used for arrhythmia classification in recent researches. The dataset contains 48 half-hour two-channel ECG recordings digitized at 11 bit resolution in 10 mV range and a rate of 360 samples per second per channel. Two cardiologists annotated each record separately (about 110,000 annotations in total). MIT-BIH has annotated 41 categories which can be converted to five-classes classification problems following the ANSL/AAMI EC57: 2012 (The Association for the Advancement of Medical Instrumentation) standard. These distinctive classes are: Normal Sinus Rhythm (N), Supraventricular Premature or Ectopic Beat (S), Ventricular Premature or Ectopic Beat (V), Fusion of Ventricular and Normal Beat (F), Unknown Beats (Q). Some researches were carried on three or four classes due to imbalanced sample size, making the comprehensive evaluation difficult. In this paper, we chose to adapt to all the five classes.

4.3.2. PTB Diagnostic ECG Database

The PTB diagnostic ECG database is a popular ECG recording database collected by the National Metrology Institute of Germany Boussejot et al. (1995). The dataset contains 549 records from 290 subjects (aged 17 to 87, mean 57.2; 209 men, mean age 55.5, and 81 women, mean age 61.6; ages were not recorded for 1 female and 14 male subjects). Each subject is represented by one to five records. Each record includes 15 simultaneously measured signals: the conventional 12 leads (i, ii, iii, avr, avl, avf, v1, v2, v3, v4, v5, v6) together with the 3 Frank lead ECGs (vx, vy, vz). Each signal is digitized at 1000 samples per second, with 16 bit resolution over a range of ± 16.384 mV. The PTB dataset consists of two main classes, i.e., (1) Normal (N), which represents normal ECG recordings, and (2) the Myocardial Infarction (M), which represents ECG recordings that exhibit signs of myocardial infarction, indicating the presence of a heart attack.

5. Experimental Results

5.1. Performance Evaluation

Many previous work focused on only four or less classes performance, aiming to reduce the perplexity of the problem or concentrate on specific arrhythmia types. However, it leads to great difficulties to compare the ability and universality of different models. In our work, we operate our evaluation on five full classes.

Table 1

The detailed description of adopted datasets.

Database	MIT-BIH Arrhythmia						PTB		
	Classes	N	S	V	F	Q	Total	Normal	Abnormal
Training	72470	2223	5788	641	6431	87553	3236	8400	11636
Testing	18117	556	1448	162	1608	21891	809	2100	2909

Table 3

The detailed results for each class on MIT-BIH dataset.

Metrics	Per-class performance					Macro-Avg
	N	S	V	F	Q	
Accuracy	99.03	99.21	99.74	99.77	99.94	99.54
Sensitive	99.86	72.12	98.20	75.31	99.56	89.01
F1-score	99.44	83.52	98.96	85.29	99.75	93.50
Precision	98.98	95.70	97.80	91.73	99.56	96.76
Specificity	95.07	99.92	99.84	99.95	99.97	98.95

Table 2

Confusion matrix of model prediction on MIT-BIT dataset

	N	S	V	F	Q
N	18092	11	14	0	1
S	153	401	1	0	1
V	3	7	1422	11	5
F	29	0	11	122	0
Q	1	0	6	0	1601

Table 2 shows the confusion matrix of our best model prediction. And the detailed evaluations on each class of the MIT-BIH dataset are presented in Table3. The result shows our model has excellent ability of discrimination, especially in class N, V and Q the Sensitive, Precision and Specificity reached almost 100%, which can be attribute the large training sample size. The performance of Supraventricular Premature or Ectopic Beat (S) is not so outstanding, which can be the result of lack of training samples and the Fusion of Ven-tricular. The average performance of Normal Beat (F) can be the reason its original features resemble to the Normal class (N).

Table 4

Confusion matrix of model prediction on PTB dataset

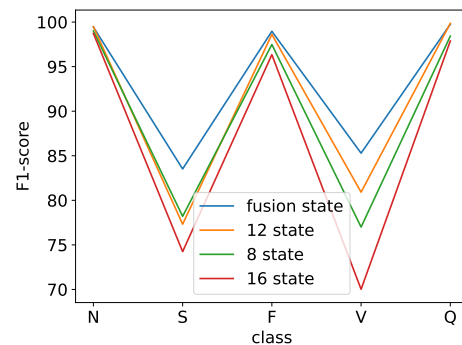
	N	M
N	800	9
M	4	2096

Table 5

The detailed results for each class on PTB dataset.

Metrics	Per-class performance		Macro-Avg
	N	M	
Accuracy	99.59	99.59	99.59
Sensitive	99.24	99.72	99.48
F1-score	98.89	99.86	99.37
Precision	99.63	99.57	99.60
Specificity	99.86	98.89	99.37

Table 4 and Table 5 also show our model great performance on PTB dataset. The confusion matrix indicates that our model predicts nearly all of positive and Negative samples, with an macro-avg accuracy of 99.59%.

**Figure 3:** The F1-score of different states

The performance of our model is also compared with several previous studies, which is presented in Table 6, presenting comparative advantages over the other architectures. And the performance of each label can be seen in Table 7, which can be observed from the result that our model has

Table 6

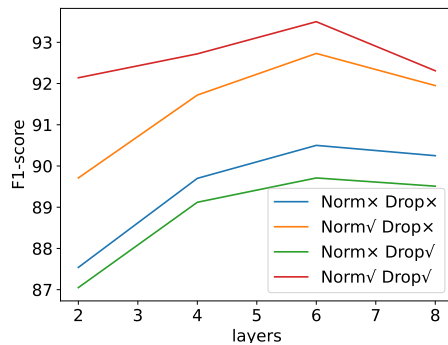
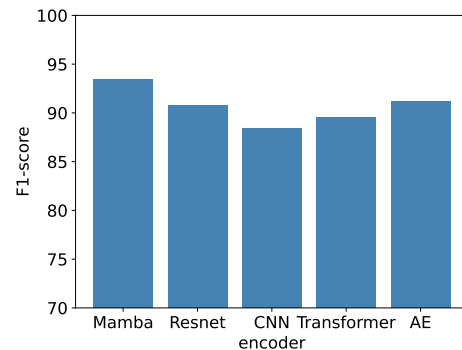
Comparison of models with different architectures on MIT-BIH dataset

Baseline	Methods	Accuracy	F1-score
Ours	Mamba + Capsule Networks	99.54	93.50
El-Ghaish and Eldele (2024)	MSC + CRM + BiTrans + CAL	99.35	94.26
Xia et al. (2023)	CNN + DAE + Transformer	97.66	-
Nurmaini et al. (2020)	DAE + DNN	99.34	91.44
Jin et al. (2021)	DLA + CLSTM	88.76	80.54
Kim et al. (2022)	ResNet+ SE block + biLSTM	99.20	91.69
Hammad et al. (2020)	ResNet + LSTM + GA	98.00	89.70
Sellami and Hwang (2019)	CNN	95.33	80.08
Pokaprakarn et al. (2021)	Seq2Seq + CRNN	97.60	89.00

Table 7

Comparison of performance of labels on MIT-BIH dataset

Baseline	Acc	N			S			V			F			Q		
		SEN	PPV	SPEC	SEN	PPV	SPEC	SEN	PPV	SPEC	SEN	PPV	SPEC	SEN	PPV	SPEC
Ours	99.54	99.86	98.98	95.07	72.12	95.70	99.92	98.20	97.80	99.84	75.31	91.73	99.95	99.56	99.56	99.97
El-Ghaish and Eldele (2024)	99.35	99.46	99.36	-	86.91	91.67	-	97.65	95.74	-	82.68	91.30	-	99.06	99.30	-
Xia et al. (2023)	97.66	97.35	96.47	71.09	70.26	82.90	99.44	73.92	71.67	96.42	13.40	30.41	99.08	0.00	0.00	99.98
Hammad et al. (2020)	98.00	98.40	99.40	95.30	90.00	79.10	99.20	95.10	91.80	99.30	88.80	91.10	99.70	33.30	25.00	99.90
Acharya et al. (2017)	97.37	91.64	85.17	96.01	89.04	94.76	98.77	94.07	95.05	98.74	95.21	94.69	98.67	97.39	98.40	99.61
Sellami and Hwang (2019)	95.33	88.51	98.80	91.30	82.04	30.44	92.80	92.05	72.13	97.54	68.30	26.58	98.52	14.29	50.00	95.33
Marinho et al. (2019)	94.30	99.00	-	57.60	2.70	-	99.80	87.80	-	99.40	49.50	-	99.60	0.00	-	94.30
Li et al. (2019b)	91.44	91.81	98.92	91.65	95.15	90.11	93.62	89.05	35.41	99.21	32.22	20.36	98.93	0.00	-	91.44
Chen et al. (2020)	96.77	99.15	97.81	81.96	63.90	76.10	99.23	88.84	96.78	99.80	47.68	54.25	99.68	-	-	-
Wang et al. (2020)	96.72	95.05	98.35	87.07	90.25	43.50	95.50	84.13	89.52	99.32	1.29	5.32	99.82	-	-	-
Shi et al. (2019)	92.07	92.13	99.45	95.64	91.67	46.22	95.51	95.12	88.09	99.04	61.60	15.16	97.12	-	-	-
Dias et al. (2021)	90.29	79.64	99.51	98.09	91.32	40.34	94.81	87.26	93.15	99.55	81.14	4.50	86.24	-	-	-

**Figure 4:** The F1-score of different layers**Figure 5:** The F1-score with different encoders.

considerable advantages compared with others in majority classes.

5.2. Ablation Study

The ablation experiment was carried out to test the effectiveness of our model structure. Since **Mamba** was mainly used as the encoder and capsule networks as the decoder in our model, the ablation experiment was carried out in these two aspects on MIT-BIH dataset.

5.2.1. Encoder Structure

This experiment aims to compare the performance of different model structures, including the number of stacked

mamba layers, the number of mamba states, the steps per layer, whether to adopt the layernorm and dropout structures, and the use of different models as encoders.

In order to assess the number of mamba states and steps in each layer, we adjusted these parameters while keeping the encoder layers fixed at 4. The experimental results depicted in the figure3 demonstrate a significant impact of varying numbers of states and steps on the outcomes. Moreover, a layer composed of diverse mamba blocks outperforms a single layer due to its ability to focus on different ECG data features across various time scales. Consequently, this wider temporal coverage achieved by combined blocks leads to

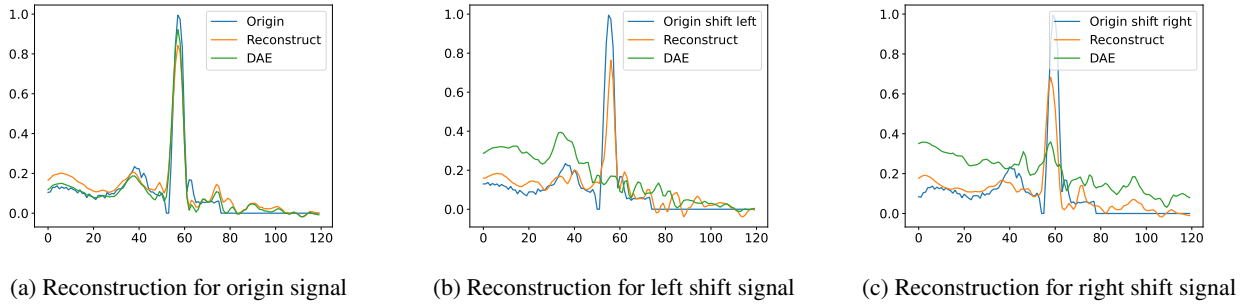


Figure 6: Disturbance reconstruction

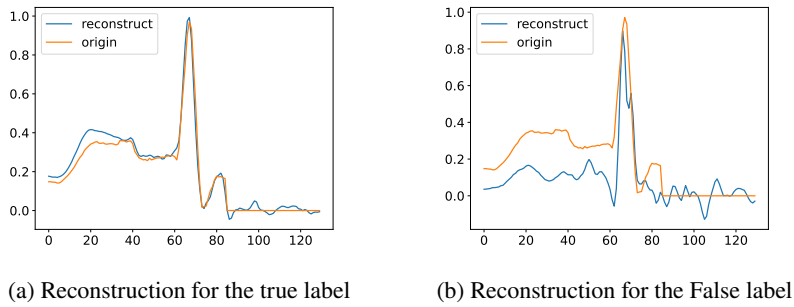


Figure 7: Different types reconstruction

enhanced performance. However, if the states are too wide it will miss significant information.

To assess the impact of encoder layers on model performance, we held the parameters of each layer constant and varied the number of encoder layers from 2 to 8 while considering whether to implement layer normalization and dropout. The corresponding results are depicted in the figure 4. From our analysis of training time and memory usage for a four-layer encoder, it is evident that the metric increases with additional layers; however, model performance does not improve proportionally with increased depth. In fact, the optimal performance is achieved at six layers due to limitations in information capacity exceeding what can be learned from available data as well as increased computational demands associated with larger models.

In order to evaluate the effect of different types of encoder, we have also tried to use resnet, transformer and cnn as encoders. The experimental results are shown in the figure 5. The results show that mamba has the best effect when it is used as encoder.

5.2.2. Decoder Structure

The purpose of this experiment was to compare the changes in the model training and the performance caused by using capsule instead of traditional decoder.

We tried to replace the capsule network with MLP after freezing encoder parameters. Experiments showed that there was no significant difference between the capsule network and MLP under the same encoder with F1-score 93.50

compared to 93.62, but the training time of capsule network was longer than that of MLP. This is determined by the routing structure of the capsule network and the number of parameters.

5.3. Explainable Study

The interpretability of this paper is unique from other recent papers on ECG diagnosis, mainly through the reconstruction of ECG signals in different ways to explain what knowledge the model has learned on MIT-BIH dataset. For the reason of the limitation of the memory, we only consider P-wave and R-wave in our reconstruction, discarding the T-wave which is far from the center of the signal.

5.3.1. Feature Relation Mining

When processing the ECG graphs, the human brain not only attends to focus on individual wave peaks but also considers the interrelationship between them. The view invariance of capsule network aligns remarkably well with this characteristic, which is why we selected it as the decoder. In our experiment, we conducted forward and backward disturbance on the input data to observe the disturbance reconstruction of ECG signals using our model and DAE model. The experimental results are depicted in the figure 6, where left and right shift represent forward and backward shift respectively. Repeated reconstructions of ECG signals by MambaCapsule exhibit remarkable consistency, indicating that Mambacapsule has learned not only the intrinsic features but also their interrelationships. Conversely, this

characteristic is absent in the reconstructed ECG signal produced by DAE model.

5.3.2. Cardiac Disease Manifestation Type Inspection

When human brain categorize an item, it can discern the reasons for its classification and differentiation. Due to the inherent output characteristics of Capsule network, the output not only encompasses the probability density of each category but also encapsulates the distinctive features associated with that particular category. Consequently, by reconstructing ECG signals from unified inputs belonging to different categories, we are able to precisely comprehend why the model deems a certain category more probable. The experimental results are depicted in Figure 7. In Figure 7a, both the ECG signal and model prediction are labeled as N, where P, R wave can be observed clearly and can be distinguished it represents a normal signal. However in Figure 7b, which is reconstructed by the label S and the length of the capsule is adjusted to be equal to the capsule of label N. The false reconstruction represents a vanish in P-wave, which is a symbol of Supraventricular Premature or Ectopic Beat. The reconstructions of N and P labels demonstrate an ability of knowledge explanation and thus, each capsule can be seen as the information collection of different labels and the length of it is how much the information is concluded in the signal.

6. Conclusion

In this work, we have proposed an effective-while-explainable solution to ECG classification by introducing MambaCapsule, which emphasizes the capability of multi-scale Mamba in feature extracting and the interpretability of the form of Capsule network. By applying evaluation and reconstruction, the result of our model reveals great advantages in both classification score and mechanism explainability. However, it's necessary to realize the limitation of our model, a the long training time and big memory occupied. In our future work, we aim to address these challenges by applying pre-trained parameters and optimize routing structure in Capsule network. As an automatic heart rhythm abnormality detection system, our model can offer doctors and patients accurate and reliable results, which have a wide range of application prospects.

References

Acharya, U.R., Oh, S.L., Hagiwara, Y., Tan, J.H., Adam, M., Gertych, A., San Tan, R., 2017. A deep convolutional neural network model to classify heartbeats. *Computers in biology and medicine* 89, 389–396.

Bao, M., Huang, C., Wang, L., Zhang, T., Jiang, Y., 2017. Visual information processing and its brain mechanism. *Sci. Technol. Rev* 35, 15–20.

Bian, Y., Chen, J., Chen, X., Yang, X., Chen, D.Z., Wu, J., 2022. Identifying electrocardiogram abnormalities using a handcrafted-rule-enhanced neural network. *IEEE/ACM Transactions on Computational Biology and Bioinformatics* 20, 2434–2444.

Bousseljot, R., Kreiseler, D., Schnabel, A., 1995. Nutzung der ekg-signaldatenbank cardiodat der ptb über das internet .

Chen, A., Wang, F., Liu, W., Chang, S., Wang, H., He, J., Huang, Q., 2020. Multi-information fusion neural networks for arrhythmia automatic detection. *Computer methods and programs in biomedicine* 193, 105479.

Chen, J., Huang, S., Zhang, Y., Chang, Q., Zhang, Y., Li, D., Qiu, J., Hu, L., Peng, X., Du, Y., et al., 2024. Congenital heart disease detection by pediatric electrocardiogram based deep learning integrated with human concepts. *Nature Communications* 15, 976.

Chen, J., Liao, K., Fang, Y., Chen, D., Wu, J., 2023. Tabcaps: A capsule neural network for tabular data classification with bow routing. in: *The Eleventh International Conference on Learning Representations*.

Chen, J., Liao, K., Wei, K., Ying, H., Chen, D.Z., Wu, J., 2022. MEGAN: Learning panoptic electrocardio representations for multi-view ecg synthesis conditioned on heart diseases. in: *International Conference on Machine Learning*, PMLR. pp. 3360–3370.

Chen, J., Yu, H., Qian, C., Chen, D.Z., Wu, J., 2021a. A receptor skeleton for capsule neural networks. in: *International Conference on Machine Learning*, PMLR. pp. 1781–1790.

Chen, J., Zheng, X., Yu, H., Chen, D.Z., Wu, J., 2021b. Electrocardio panorama: synthesizing new ecg views with self-supervision. *arXiv preprint arXiv:2105.06293* .

Dias, F.M., Monteiro, H.L., Cabral, T.W., Naji, R., Kuehni, M., Luz, E.J.d.S., 2021. Arrhythmia classification from single-lead ecg signals using the inter-patient paradigm. *Computer Methods and Programs in Biomedicine* 202, 105948.

El-Ghaish, H., Eldele, E., 2024. Ecgrtransform: Empowering adaptive ecg arrhythmia classification framework with bidirectional transformer. *Biomedical Signal Processing and Control* 89, 105714.

Faust, O., Martis, R.J., Min, L., Zhong, G.L.Z., Yu, W., 2013. Cardiac arrhythmia classification using electrocardiogram. *J. Med. Imaging Health Inf* 3, 448.

Gu, A., 2023. Modeling Sequences with Structured State Spaces. Stanford University.

Gu, A., Dao, T., 2023. Mamba: Linear-time sequence modeling with selective state spaces. *arXiv preprint arXiv:2312.00752* .

Gu, A., Dao, T., Ermon, S., Rudra, A., Ré, C., 2020. Hippo: Recurrent memory with optimal polynomial projections. *Advances in neural information processing systems* 33, 1474–1487.

Gu, A., Goel, K., Ré, C., 2021. Efficiently modeling long sequences with structured state spaces. *arXiv preprint arXiv:2111.00396* .

Hammad, M., Ilyyasu, A.M., Subasi, A., Ho, E.S., Abd El-Latif, A.A., 2020. A multitier deep learning model for arrhythmia detection. *IEEE Transactions on Instrumentation and Measurement* 70, 1–9.

Hong, S., Xiao, C., Ma, T., Li, H., Sun, J., 2019. Mina: multilevel knowledge-guided attention for modeling electrocardiography signals. *arXiv preprint arXiv:1905.11333* .

Hu, Y., Chen, J., Hu, L., Li, D., Yan, J., Ying, H., Liang, H., Wu, J., 2024. Personalized heart disease detection via ecg digital twin generation. *arXiv preprint arXiv:2404.11171* .

Jin, Y., Liu, J., Liu, Y., Qin, C., Li, Z., Xiao, D., Zhao, L., Liu, C., 2021. A novel interpretable method based on dual-level attentional deep neural network for actual multilabel arrhythmia detection. *IEEE Transactions on Instrumentation and Measurement* 71, 1–11.

Khraishah, H., Alahmad, B., Ostergard Jr, R.L., AlAshqar, A., Albaghdadi, M., Vellanki, N., Chowdhury, M.M., Al-Kindi, S.G., Zamboni, A., Gasparrini, A., et al., 2022. Climate change and cardiovascular disease: implications for global health. *Nature Reviews Cardiology* 19, 798–812.

Kim, Y.K., Lee, M., Song, H.S., Lee, S.W., 2022. Automatic cardiac arrhythmia classification using residual network combined with long short-term memory. *IEEE Transactions on Instrumentation and Measurement* 71, 1–17.

Krittanawong, C., Zhang, H., Wang, Z., Aydar, M., Kitai, T., 2017. Artificial intelligence in precision cardiovascular medicine. *Journal of the American College of Cardiology* 69, 2657–2664.

Li, C., Quan, C., Peng, L., Qi, Y., Deng, Y., Wu, L., 2019a. A capsule network for recommendation and explaining what you like and dislike. in: *Proceedings of the 42nd international ACM SIGIR conference on research and development in information retrieval*, pp. 275–284.

- Li, F., Xu, Y., Chen, Z., Liu, Z., 2019b. Automated heartbeat classification using 3-d inputs based on convolutional neural network with multi-fields of view. *IEEE Access* 7, 76295–76304.
- Li, K., Li, X., Wang, Y., He, Y., Wang, Y., Wang, L., Qiao, Y., 2024. Videomamba: State space model for efficient video understanding. *arXiv preprint arXiv:2403.06977*.
- Li, Z., Zhou, D., Wan, L., Li, J., Mou, W., 2020. Heartbeat classification using deep residual convolutional neural network from 2-lead electrocardiogram. *Journal of electrocardiology* 58, 105–112.
- Liu, J., Yang, H., Zhou, H.Y., Xi, Y., Yu, L., Yu, Y., Liang, Y., Shi, G., Zhang, S., Zheng, H., et al., 2024. Swin-umamba: Mamba-based unet with imagenet-based pretraining. *arXiv preprint arXiv:2402.03302*.
- Luppi, A.I., Rosas, F.E., Mediano, P.A., Menon, D.K., Stamatakis, E.A., 2024. Information decomposition and the informational architecture of the brain. *Trends in Cognitive Sciences*.
- Luz, E.J.d.S., Schwartz, W.R., Cámara-Chávez, G., Menotti, D., 2016. Ecg-based heartbeat classification for arrhythmia detection: A survey. *Computer methods and programs in biomedicine* 127, 144–164.
- Ma, J., Li, F., Wang, B., 2024. U-mamba: Enhancing long-range dependency for biomedical image segmentation. *arXiv preprint arXiv:2401.04722*.
- Majeed, R.R., Alkhafaji, S.K., 2023. Ecg classification system based on multi-domain features approach coupled with least square support vector machine (ls-svm). *Computer Methods in Biomechanics and Biomedical Engineering* 26, 540–547.
- Marinho, L.B., de MM Nascimento, N., Souza, J.W.M., Gurgel, M.V., Rebouças Filho, P.P., de Albuquerque, V.H.C., 2019. A novel electrocardiogram feature extraction approach for cardiac arrhythmia classification. *Future Generation Computer Systems* 97, 564–577.
- Moody, G.B., Mark, R.G., 2001. The impact of the mit-bih arrhythmia database. *IEEE engineering in medicine and biology magazine* 20, 45–50.
- Nguyen, H.H., Yamagishi, J., Echizen, I., 2019. Use of a capsule network to detect fake images and videos. *arXiv preprint arXiv:1910.12467*.
- Nurmaini, S., Darmawahyuni, A., Sakti Mukti, A.N., Rachmatullah, M.N., Firdaus, F., Tutuko, B., 2020. Deep learning-based stacked denoising and autoencoder for ecg heartbeat classification. *Electronics* 9, 135.
- Nurmaini, S., Umi Partan, R., Caesarendra, W., Dewi, T., Naufal Rahmatullah, M., Darmawahyuni, A., Bhayyu, V., Firdaus, F., 2019. An automated ecg beat classification system using deep neural networks with an unsupervised feature extraction technique. *Applied sciences* 9, 2921.
- Pokaprakarn, T., Kitzmiller, R.R., Moorman, R., Lake, D.E., Krishnamurthy, A.K., Kosorok, M.R., 2021. Sequence to sequence ecg cardiac rhythm classification using convolutional recurrent neural networks. *IEEE journal of biomedical and health informatics* 26, 572–580.
- Pyakillya, B., Kazachenko, N., Mikhailovsky, N., 2017. Deep learning for ecg classification, in: *Journal of physics: conference series*, IOP Publishing. p. 012004.
- Qiao, Y., Yu, Z., Guo, L., Chen, S., Zhao, Z., Sun, M., Wu, Q., Liu, J., 2024. VI-mamba: Exploring state space models for multimodal learning. *arXiv preprint arXiv:2403.13600*.
- Qin, Q., Li, J., Zhang, L., Yue, Y., Liu, C., 2017a. Combining low-dimensional wavelet features and support vector machine for arrhythmia beat classification. *Scientific reports* 7, 6067.
- Qin, Q., Li, J., Zhang, L., Yue, Y., Liu, C., 2017b. Combining low-dimensional wavelet features and support vector machine for arrhythmia beat classification. *Scientific reports* 7, 6067.
- Ribeiro, A.H., Ribeiro, M.H., Paixão, G.M., Oliveira, D.M., Gomes, P.R., Canazart, J.A., Ferreira, M.P., Andersson, C.R., Macfarlane, P.W., Meira Jr, W., et al., 2020. Automatic diagnosis of the 12-lead ecg using a deep neural network. *Nature communications* 11, 1760.
- Rimon, Z., Jurgenson, T., Krupnik, O., Adler, G., Tamar, A., 2024. Mamba: an effective world model approach for meta-reinforcement learning. *arXiv preprint arXiv:2403.09859*.
- Rouhi, R., Clausel, M., Oster, J., Lauer, F., 2021. An interpretable hand-crafted feature-based model for atrial fibrillation detection. *Frontiers in Physiology* 12, 657304.
- Sabour, S., Frosst, N., Hinton, G.E., 2017. Dynamic routing between capsules. *Advances in neural information processing systems* 30.
- Sellami, A., Hwang, H., 2019. A robust deep convolutional neural network with batch-weighted loss for heartbeat classification. *Expert Systems with Applications* 122, 75–84.
- Shahroudjed, A., Afshar, P., Plataniotis, K.N., Mohammadi, A., 2018. Improved explainability of capsule networks: Relevance path by agreement, in: *2018 IEEE global conference on signal and information processing (GlobalSIP)*, IEEE. pp. 549–553.
- Shi, H., Wang, H., Huang, Y., Zhao, L., Qin, C., Liu, C., 2019. A hierarchical method based on weighted extreme gradient boosting in ecg heartbeat classification. *Computer methods and programs in biomedicine* 171, 1–10.
- Vijayakumar, T., 2019. Comparative study of capsule neural network in various applications. *Journal of Artificial Intelligence* 1, 19–27.
- Wang, C., Tsepa, O., Ma, J., Wang, B., 2024a. Graph-mamba: Towards long-range graph sequence modeling with selective state spaces. *arXiv preprint arXiv:2402.00789*.
- Wang, H., Shi, H., Lin, K., Qin, C., Zhao, L., Huang, Y., Liu, C., 2020. A high-precision arrhythmia classification method based on dual fully connected neural network. *Biomedical Signal Processing and Control* 58, 101874.
- Wang, J., Chen, J., Chen, D., Wu, J., 2024b. Large window-based mamba unet for medical image segmentation: Beyond convolution and self-attention. *arXiv preprint arXiv:2403.07332*.
- Wang, R., Liu, M., Cheng, X., Wu, Y., Hildebrandt, A., Zhou, C., 2021. Segregation, integration, and balance of large-scale resting brain networks configure different cognitive abilities. *Proceedings of the National Academy of Sciences* 118, e2022288118.
- Xia, Y., Xiong, Y., Wang, K., 2023. A transformer model blended with cnn and denoising autoencoder for inter-patient ecg arrhythmia classification. *Biomedical Signal Processing and Control* 86, 105271.
- Xiang, C., Zhang, L., Tang, Y., Zou, W., Xu, C., 2018. Ms-capsnet: A novel multi-scale capsule network. *IEEE Signal Processing Letters* 25, 1850–1854.
- Xinyi, Z., Chen, L., 2018. Capsule graph neural network, in: *International conference on learning representations*.
- Yan, G., Liang, S., Zhang, Y., Liu, F., 2019. Fusing transformer model with temporal features for ecg heartbeat classification, in: *2019 IEEE International Conference on Bioinformatics and Biomedicine (BIBM)*, IEEE. pp. 898–905.
- Yıldırım, Ö., Pławiak, P., Tan, R.S., Acharya, U.R., 2018. Arrhythmia detection using deep convolutional neural network with long duration ecg signals. *Computers in biology and medicine* 102, 411–420.
- Zhao, Y., Birdal, T., Deng, H., Tombari, F., 2019. 3d point capsule networks, in: *Proceedings of the IEEE/CVF conference on computer vision and pattern recognition*, pp. 1009–1018.
- Zhu, L., Liao, B., Zhang, Q., Wang, X., Liu, W., Wang, X., 2024. Vision mamba: Efficient visual representation learning with bidirectional state space model. *arXiv preprint arXiv:2401.09417*.